Marine target detection using dual−polarimetric SAR imagery

ZHANG Tao [1], MARINO Armando[2], NUNZIATA Ferdinando[3], VELOTTO Domenico[4], SHAO Weizeng[5], LI Xiaofeng[6], MIGLIACCIO Maurizio[3], XIONG Huilin[1]

1. *School of Electronic Information and Electrical Engineering, Shanghai Jiao Tong University, Shanghai,* 200240*, China*;
2. *The University of Stirling, Natural Sciences, Stirling, FK*9 4*LA, U.K.*;
3. *Università degli Studi di Napoli Parthenope, Napoli,* 38-80133*, Italy*;
4. *German Aerospace Center, Bremen,* 28199*, Germany*;
5. *Marine Science and Technology College, Zhejiang Ocean University,* 316022*, Zhoushan, China*;
6. *GST at NOAA/NESDIS, College Park, Maryland,* 20742*, USA*

Abstract: In this study, we provide a summary of research advances in the field of maritime target detection using DP (dual-polarimetric) SAR (Synthetic Aperture Radar) imagery, accomplished during the European and China collaboration in the framework of the Dragon-4 program ID 32235. The main innovative contribution is twofold: a) we addressed ship detection proposing an improved GP-PNF (Geometrical Perturbation – Polarimetric Notch Filter), termed as IGP-PNF, that is characterized by a new feature vector that includes three new scattering features; b) we addressed oil platform detection by contrasting single-polarization SAR methods with polarimetric ones in order to quantify the extra- benefit carried on polarimetric information. The proposed theoretical framework is tested against actual multi-polarization SAR data. In particular, ship detection methods are verified against a Sentinel-1 SAR scene where a large number of ship is present; while, oil platform detection is discussed using TerraSAR-X SAR data. Experimental analysis show that: (1) the IGP-PNF method performs best in terms of clutter-to-target ratio; (2) coherent polarimetric information significantly outperforms single-polarization SAR measurements in highlighting targets in challenging cases.

Key words: marine target detection, dual-polarimetric SAR, GP-PNF, PCA, Sentinel-1, TS-X

Citation format: Zhang T,Marino A,Nunziata F,Velotto D,Shao W Z,Li X F,Migliaccio M and Xiong H L. 2020. Marine target detection using dual−polarimetric SAR imagery. Journal of Remote Sensing(Chinese). 24(S1): 104−109

1 INTRODUCTION

With the development of marine traffic, the number of man-made targets, such as ships and oil platforms, have increased greatly. Meanwhile, illegal activities such as smuggling, illegal fishing, and illegal immigration also become problematic [1]. In order to protect the safety of sea activities, the surveillance of marine targets has become an important issue for many coastal countries [2]. Within this context, the SAR (Synthetic Aperture Radar) has been widely used for earth observation due to its ability to image at day-and-night almost independently of weather condition. Especially, object detection using SAR imagery attracted large attention in recent years. However, the backscattering produced by high oceanic state and speckle noise make object detection using SAR imagery a challenging task [3]. On this purpose, multi-polarization SAR (PolSAR) data can help enhance the scattering differences between marine targets and sea clutter. PolSAR configurations can provide much details on the observed scattering scene than single-polarization SAR configurations. PolSAR measurements are usually represented by the scattering matrix [*S*] [4]:

$$[S] = \begin{bmatrix} S_{HH} & S_{HV} \\ S_{VH} & S_{VV} \end{bmatrix} \quad (1)$$

where, for instance, S_{HV} denotes the horizontal receiving and vertical transmitting polarization channel. Under reciprocity conditions, the [*S*] scattering matrix is symmetrical, i.e.; $S_{HV}=S_{VH}$.

In the earlier studies, ship detection has been mainly tackled using single-polarization SAR imagery processed according to CFAR (Constant False Alarm Rate) schemes [5] [6]. Recently, Pappas *et al*. [7] proposed a superpixel-level CFAR method for ship detection, which shows a better detection performance than some classical CFAR detectors. In fact, these CFAR-based approaches greatly depend on the background clutter distribution. Thus, their detection performance may degrade rapidly in the heterogenous areas where the statistical characteristics difference between the sea surface and ship is not large [3].

When dealing with PolSAR approaches, the first attempts to exploit polarimetric information were based on: data fusion among the different polarimetric channels; the scattering power detectors,

Received: 2019-10-21; **Accepted:** 2020-04-16

Foundation: ESA-NRSCC Dragon-4 project ID 32235

First author biography: ZHANG Tao (1989—), male, a PhD Candidate. His research interest focuses on PolSAR Image processing and machine learning. E-mail: sjtu--zt@sjtu.edu.cn

e.g., the SPAN (Total Power) detector, PWF (Polarimetric Whitening Filter) [8], and the power maximization detector [9]. However, although power-based methods can detect ships, they may loss effectiveness when ships have weak backscattered intensity. Hence, to fully exploit polarimetric information, inter-channel phase is needed. Within this context, several approaches have been proposed. In [10], two scattering-based algorithms, computed from Yamaguchi Polarimetric Decomposition (PD), were proposed for ship detection. Cloude et al. [11] used the entropy and α angle that are both calculated from the Cloude–Pottier decomposition to detect ships successfully. Nunziata et al. [12] exploited the RS (Reflection Symmetry) characteristic of the sea clutter to detect man-made objects at sea. Similarly, based on the dual-pol SAR data and different polarimetric models, Shirvany et al [13] utilized the degree of depolarization (DoD) for detecting man-made objects at sea. Marino et al. [14] [15] proposed a new detector, i.e., GP-PNF (Geometrical Perturbation – Polarimetric Notch Filter) for object detection by using the Huynen fork, which extracted the target features in the polarimetric target complex space.

In the context of Dragon 4 program ID 32235, we addressed ship and oil platform detection by developing tailored algorithms. In detail, one algorithm is developed for ship detection that improves the GP-PNF by introducing a new features vector. Two metrics are proposed to detect oil platforms that aim at demonstrating the superiority of PolSAR with respect to single-polarimetric methods in enhancing oil platforms even under challenging conditions. Experiments, undertaken on actual DP SAR scenes collected by Sentinel-1 and TerraSAR-X, demonstrate the soundness of the proposed rationale.

The rest of the paper is organized as follows. Section II presents the proposed algorithm and metrics. The experimental results are given in Section III. Finally, Section IV concludes the paper.

2 THE PROPOSED ALGORITHMS FOR MARINE TARGET DETECTION

2.1 Theoretical background

When dealing with distributed targets, the 3×3 coherence/covariance matrix derived from [S] is often adopted [4] as second-order descriptor. In this paper, we select the covariance matrix [C] to construct our methods.

For the dual-pol case, the scattering matrix [S] can be simplified as a column vector $\underline{k}_{dual} = [\underline{k}_{d1}, \underline{k}_{d2}]$ [13]. The element k_{d1} and k_{d2} respectively indicate the polarimetric scattering elements obtained from [S]. Conventionally, $\underline{k}_{dual}$ can be constructed using three different combinations of scattering amplitudes: $\underline{k}_{dual} = [S_{HH}, S_{HV}]$, $\underline{k}_{dual} = [S_{VH}, S_{VV}]$ or $\underline{k}_{dual} = [S_{HH}, S_{VV}]$. Then, the dual-pol covariance matrix [C_{dual}] is defined as:

$$C_{dual} = \left\langle \underline{k}_{dual} \cdot \underline{k}_{dual}^{H} \right\rangle = \begin{bmatrix} C_{dual}11 & C_{dual12} \\ C_{dual21} & C_{dual22} \end{bmatrix} \tag{2}$$

2.2 An improved GP-PNF method (IGP-PNF) for ship detection

GP-PNF is proposed by Marino et al. [14] [15] and it is an adaptation of GPF (Geometrical Perturbation Filter) to work as a notch filter in the polarimetric space. Extensive experiments demonstrated the effectiveness of GP-PNF on ship detection. In GP-PNF, a partial scattering feature vector $\underline{t}$ is firstly constructed based on the dual-pol scattering vector $\underline{k}_{dual}$, i.e. ,

$$\underline{t} = \mathrm{Trace}([C_{dual}]\Psi_2) = \left[\left\langle |k_{d1}|^2 \right\rangle, \left\langle |k_{d2}|^2 \right\rangle, \left\langle k_{d1}^{*} k_{d2} \right\rangle \right]^{\mathrm{T}} \tag{3}$$

where Ψ_2 is a complete set of 2×2 basis matrix under a Hermitian inner product and $\underline{k}_{di}$ (i=1, 2) are the elements of $\underline{k}_{dual}$. After mathematical manipulations [14]—[17], the final dual-polarimetric detector is defined as:

$$\gamma = \frac{1}{\sqrt{1 + RedR\dfrac{1}{P_T}}} \tag{4}$$

where $RedR$ is a parameter called Reduction Ratio, P_C and P_T stand for the power of clutter pixels and target pixels, respectively.

Since each feature exhibits specific advantages and disadvantages in terms of detection capabilities, in this study, a new feature vector $\underline{k}_{dual}$ is proposed to further improve the performance of GP-PNF. This feature vector is augmented by three new features, namely the power feature SPAN, the multiplying amplitude feature (we call it 'MTC' here) [18], and DoD (Degree of Depolarization) [13]. Note that, we here choose the VH/VV combination as the dual polarimetric mode. Therefore, the extended vector is defined as :

$$\underline{t}' = \left[\left\langle |S_{VV}|^2 \right\rangle, \left\langle |S_{VH}|^2 \right\rangle, \left\langle |S_{VV}{}^{*} S_{VH}| \right\rangle, \left\langle SPAN \right\rangle, \left\langle MTC \right\rangle, DoD \right] \tag{5}$$

Moreover, to reduce the dimensionality of $\underline{k}_{dual}$, PCA (Principal Component Analysis) [19] is used. Thus, the new feature vector is finally constructed as [19]:

$$\underline{t}_{new} = \left[\left\langle |f_1^{PCA}|^2 \right\rangle, \left\langle |f_2^{PCA}|^2 \right\rangle, \left\langle |f_3^{PCA}|^2 \right\rangle \right] \tag{6}$$

where f_i^{PCA} (i=1, 2, 3) are the new features after the PCA operator. Then, the expression of the detector IGP-PNF is built,

$$\gamma_d = \frac{1}{\sqrt{1 + RedR\left(\dfrac{1}{\left| \underline{t}_{new}^{*T} \hat{t}_T \right|} - 1 \right)}} \tag{7}$$

here, $\hat{t}_T$ is a normalized version of the vector representing the target $\underline{t}_T$ [20].

2.3 Oil platform detection

Platforms installed in shallow water consist of vertical metallic towers sustained by submersed pylons fixed to the sea floor. Fig. 1b, shows an interpretation of the different scattering contributions for a given azimuth angle [21]. The tower's altitude can be of several tens of meters and, hence, it may result in several scattering mechanisms that, at once, generate multiple bright spots aligned along the range direction (indicated by the yellow arrows in Fig. 1a). The first mechanism is due to what is commonly referred as layover (dashed red line path in Fig. 1(b). The second mechanism is mainly caused by double reflections between the platform vertical structures and the ocean surface (dashed green line path in Fig. 1b with yellow diamonds indicating the possible point of reflections). The third mechanism accounts for triple reflections (or even higher order) between the platform and the surrounding sea surface (dashed black line path in Fig. 1(b). They could be due to the electromagnetic wave reflected off the sea, a platform structure, again on the sea and back to the sensor (see yellow diamonds along with the dashed black path in Fig. 1(b). They are located after the platform, since the path that the electromagnetic wave has to travel is longer. According to this simplistic model, these three main mechanisms make possible the detection and, hence, platform monitoring using SAR data [13] [22].

However, platform detection is not at all straightforward and the detection performance depends significantly on both incidence angle and polarization. In fact, as it will be clearer in the follows, when co-polarized channels (HH or VV) are used, some oil platforms can be hardly recognized in the SAR image plane, despite the use of fine spatial-resolution imagery. We demonstrate that, in this very challenging scenario, PolSAR has the potential to improve significantly the detection exercise. Two simple metrics are used based on the GP-PNF and the DoD detectors.

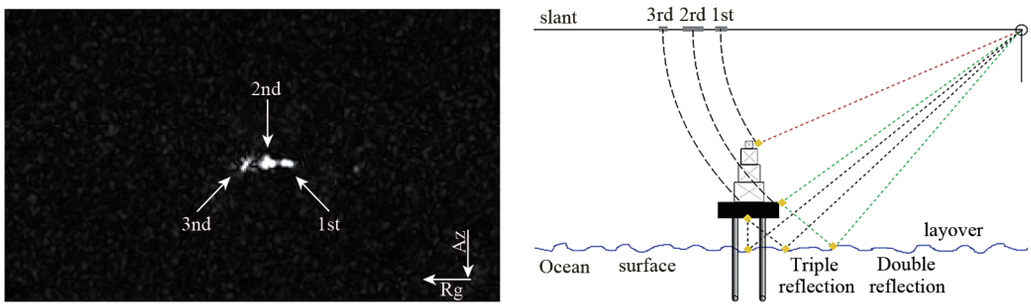

(a) TS-X WSC patch showing the typical platform backscatter signature

(b) Schematic sketch of the different signature contributions

Fig.1 Schematic sketch of the radar signatures observed in medium resolution X-band SAR data

3 EXPERIMENTS

3.1 Experimental results of IGP-PNF on Sentinel-1 data

In order to evaluate the ship detection performance of IGP-PNF, we here conduct experiments on one Sentinel-1 IW dataset with 24 real ships, which was collected in the English Channel on 12 January 2017. Note that, the oceanographic data achieved from the UK Met Office [23] shows that high sea state condition were in place. An optical (Google Earth) image along with the correspondent SAR VH amplitude image are shown in Fig.2. Two conventional detection algorithms, namely, DoD and GP-PNF are here adopted as benchmark to evaluate the performance of the proposed approach.

(a) The optical image obtained from Google Earth (Time: 2016/12/31)

(b) SAR VH amplitude image augmented with orange circles that indicate ships. The red rectangle indicates the sea clutter area used for quantitative analysis

Fig.2 The dataset

Fig.3 presents the results of these three methods. The output of DoD detector, see Fig.3a, shows that it detects few ships, while resulting in many false alarms. This is physically due to the fact that strong clutter conditions are in place that contribute to increase DoD values. Hence, the TCR (Target-Clutter-Ratio) is not large enough to obtain a remarkable performance in terms of detected targets and false alarms when DoD is used. When dealing with GP-PNF (see Fig. 3(b), it can be noted that a better performance is achieved since it detects all the ships. This is physically due to the fact that it uses more polarimetric features. In fact, for 24 ships, the average TCR of GP-PNF (10.2 dB) is 3.38 dB higher than DoD (6.82 dB). Results obtained using the IGP-PNF method are shown in Fig.3(c). It can be noted that it achieves the best performance. This is quantitatively justified by the largest average TCR value, i.e.; 12.70 dB. The reason behind the enhanced TCR value is that PCA sets the basis of the feature vector so that it aligns with the axis where the sea clutter is mostly present or less present. In addition, it moves the center of the axis in the middle of the distribution, allowing a better separation between target and clutter dimensions.

(a) DoD (b) GP-PNF (c) IGP-PNF. Red circles indicate missing ships (Yellow dashed circles stand for false alarms)

Fig.3 Ship detection results

3.2 Experimental results on TerraSAR-X data

In this subsection, two TS-X WSC mode datasets, collected at different incidence angles and polarizations are adopted. Specifically, Fig.4(a) is obtained under a low incidence angle that ranges in the interval 19.80°—21.15° (referred as *low*) and Fig.4(b) is obtained under a high incidence angle that ranges in the interval 39.15°—40.15° (referred as *high*). A reference multispectral image is also shown in false color in Fig.4(c) (band 4 in red, band 3 in green, band 2 in blue). The wind condition is similar in the two acquisitions. It is clear that, at low incidence angles, the platforms cannot be observed in the SAR imagery, despite they are tens of meters large and made by metallic structures.

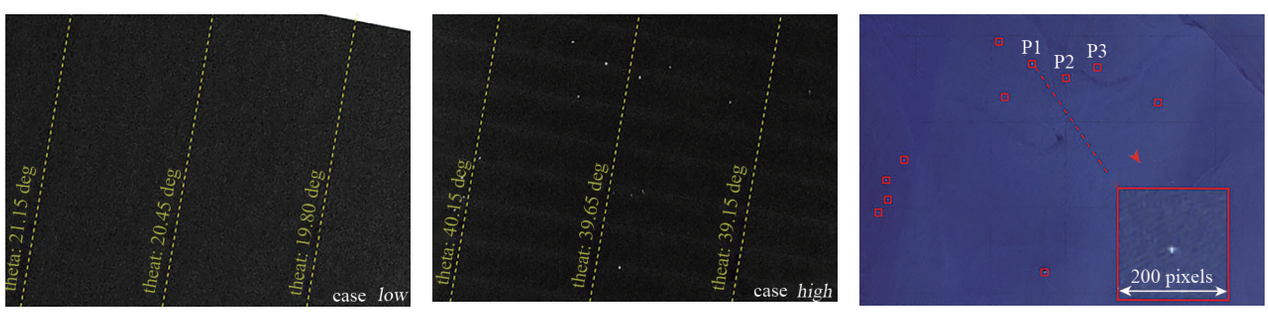

(a) The case of low incidence angle (Time: 2014/08/14) (b) The case of high incidence angle (Time: 2014/05/01) (c) The corresponding multispectral image

Fig.4 TS-X WSC Datasets

Fig.5 introduces the incoherent detection using a single polarization. It can be noted that the co-polarizations do not allow observing well-distinguishable signals associated with the platforms at low incidence angles. When other detectors are used and we perform dual pol coherent detection, we can identify some of the platforms that were missing. Note that Fig. 6 shows the results of these dual-pol detectors when combined on a single map.

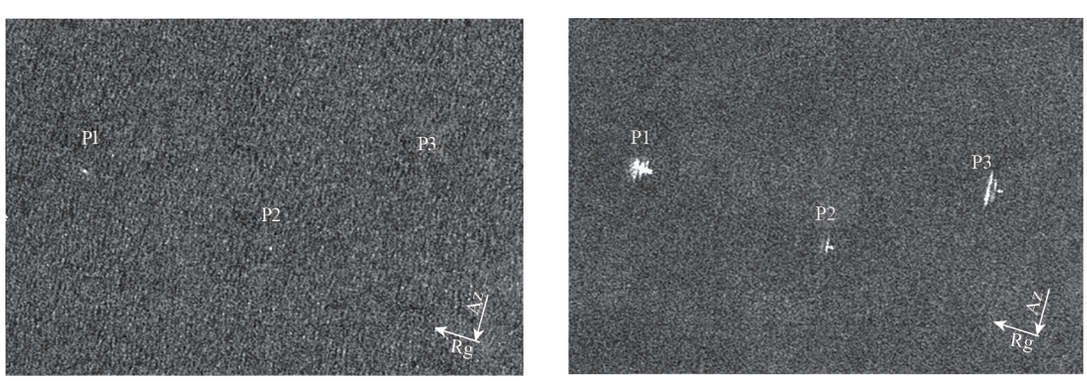

(a) HH (b) HV

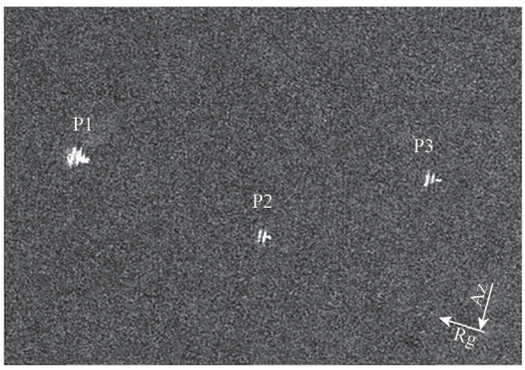

(c) VH

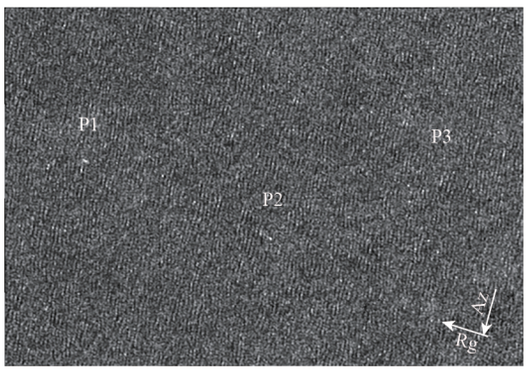

(d) VV

Fig. 5 Multi-temporal ground projected calibrated amplitude SAR data collected by TS-X/TD-X over a cluster of 3 offshore platforms in GoM (labeled as P1, P2 and P3)

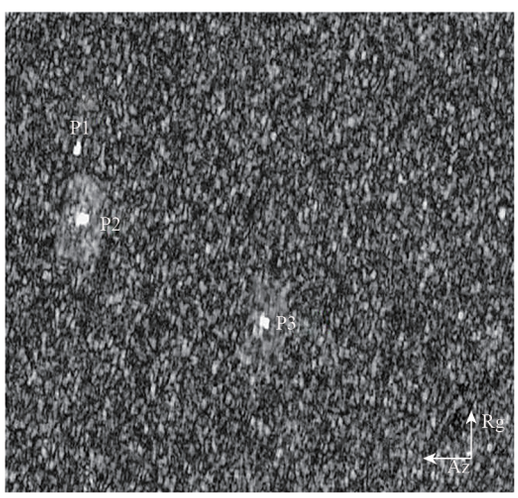

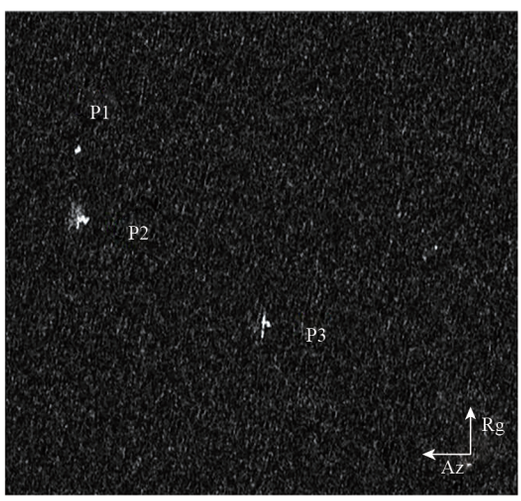

(a)—(b) ground projected and byte-scaled features PNF and DoD in correspondence of the platform P1, P2 and P3

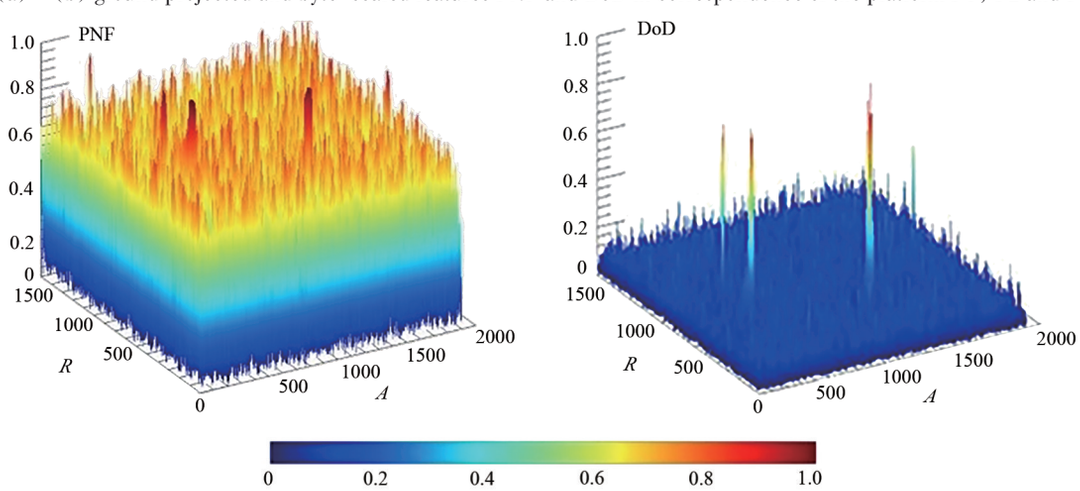

(c)—(d) Respective normalized 3D plots in satellite coordinate

Fig. 6 Case HH-VV *low* coherent analysis

4 CONCLUSIONS

This paper describes the innovative studies related to maritime target detection (i.e.; both ships and oil/gas rigs/platforms), accomplished during the Dragon 4 project ID 32235. Three algorithms designed to detect marine targets using DP SAR data were analyzed. When dealing with ship detection, we propose an improvement of the GP-PNF method (i.e., the IGP-PNF method) that consists of re-

defining the feature vector that is augmented by three polarimetric features. Then, a PCA operator is executed on the improved feature vector before applying GP-PNF. Results, obtained processing an actual Sentinel-1 dataset, show the effectiveness of IGP-PNF that results in a gain in TCR of around 2 dB with respect to conventional PolSAR methods. When dealing with oil platform detection, two metrics (i.e., GP-PNF and DoD) are developed and analyzed in this paper. Experimental results, undertaken on two TS-X datasets collected at different incidence angles and polarizations, demonstrate that, when dealing with the challenging low incidence angle case: (1) single-polarization co-polarized imagery does not show remarkable hints related to the metallic targets; (2) the coherent channel combination helps in highlighting the targets.

5 ACKNOWLEDGEMENT

This study is supported by ESA-NRSCC Dragon-4 project ID 32235 entitled "Microwave satellite measurements for coastal area and extreme weather monitoring". The authors would like to thank DLR for providing the TS-X/TD-X data via the AO project (OCE1045). Offshore platform locations in the Gulf of Mexico are provided as public information by the Bureau of Safety and Environmental Enforcement. We thanks ESA for the provision of Sentinel-1 data. It is acknowledged that Landsat-8 data has been downloaded from the United States Geological Survey website.

REFERENCES

Bueger C. 2015. What is maritime security? Mar. Policy, 53:159-164.

Brusch S, Lehner S, Fritz T, Soccorsi M, Soloviev A and van Schie B. Ship surveillance with TerraSAR-X. IEEE Trans. Geosci. Remote Sens, 49(3): 1092 – 1103.

Zhang T, Yang Z and Xiong H L. PolSAR ship detection based on the polarimetric covariance difference matrix. IEEE J. Sel. Top. Appl. Earth Obs. Remote Sens, 10(7): 3348 – 3359.

Lee J S and Pottier E. 2009. Polarimetric radar image: from basics to applications. Boca Raton, FL, USA: CRC Press.

Robey F C, Fuhrmann D R, Kelly E J and Nitzberg R. 1992. A CFAR adaptive matched filter detector. IEEE Trans. Aeros. Electron. Syst., 28(1): 208 – 216.

Wackerman C C, Friedman K S, Pichel W G, Clemente-Colón P and Li X F. 2001. Automatic detection of ships in Radarsat-1 SAR imagery. Canadian J. Remote Sens, 27(5): 568 – 577.

Pappas O, Achim A and Bull D. 2018. Superpixel-level CFAR detectors for ship detection in SAR imagery. IEEE. Geosci. Remote Sens. Letters, Early Access.

Novak L M, Burl M C and Irwing W W. 1993. Optimal polarimetric processing for enhanced target detection. IEEE Trans. Aerosp. Electron. Syst., 29(1): 234 – 243.

Chaney R D, Bud M C and Novak L M. 1990. On the performance of polarimetric target detection algorithms. IEEE Aerosp. Electron. Syst. Mag., 5(11): 10 – 15.

Sugimoto M, Ouchi K and Nakamura Y. 2013. On the novel use of model-based decomposition in SAR polarimetry for target detection on the sea. Remote Sens. Lett. 4(9): 843 – 852.

Cloude S R and Pottier E. 1997. An entropy based classification scheme for land applications of polarimetric SAR. IEEE Trans. Geosci. Remote Sens. 35(1): 68 – 78.

Nunziata F, Migliaccio M and Brown C E. 2012. Reflection symmetry for polarimetric observation of man-made metallic targets at sea. IEEE J. Ocean. Eng. 37(3): 384 – 394.

Shirvany R, Chabert M and Tourneret J Y. 2013. Ship and oil-spill detection using the degree of polarization in linear and hybrid/compact

dual-pol SAR. IEEE J. Sel. Top. Appl. Earth Obs. Remote Sens, 5(3): 885 – 892.

Marino A, Cloude S R and Woodhouse I H. 2012. Detecting depolarized targets using a new geometrical perturbation filter. IEEE Trans. Geosci. Remote Sens. 50(10): 3787 – 3799.

Marino A and Hajnsek I. 2015. Statistical tests for a ship detector based on the Polarimetric Notch Filter. IEEE Trans. Geosci. Remote Sens. 53(8): 4578 – 4595.

Marino A. 2013. A notch filter for ship detection with polarimetric SAR data. IEEE J. Sel. Top. Appl. Earth Obs. Remote Sens. 6(3): 1219 – 1232.

Marino A, Sugimoto M, Ouchi K and Hajnsek I. 2014. Validating a Notch Filter for detection of targets at sea with ALOS-PALSAR Data: Tokyo Bay. IEEE J. Sel. Top. Appl. Earth Obs. Remote Sens. 7(12): 4907 – 4918.

Hannevik T N. 2010. Polarisation and mode combinations for ship detection using radarsat-2. In Proceedings of the IEEE Geoscience and Remote Sensing Symposium (IGARSS), Honolulu, HI, USA, 3676 – 3679.

Zhang T, Marino A and Xiong H L. 2018. A Ship Detector Applying Principal Component Analysis to the Polarimetric Notch Filter. Remote Sens, 10(6): 948.

Tipping M E and Bishop C M. 2002. Probabilistic principal component analysis. J. R. Stat. Soc. 61(3): 611 – 622.

Marino A, Velotto D and Funziata F. 2017. Offshore metallic platforms observation using dual-polarimetric TS-X/TD-X satellite imagery: A case study in the Gulf of Mexico. IEEE J. Sel. Top. Appl. Earth Obs. Remote Sens. 10(10): 4376 – 4386.

Cheng L, Yang K, Tong L H, Liu Y X and Li M C. 2013. Invariant triangle-based stationary oil platform detection from multi-temporal synthetic aperture radar data. J. of Applied Remote Sens. 7(1).

Met OfficeUK. Available online: http://www.metoffice.gov.uk/public/weather.